Experimental Evidence of the Collective Brillouin Scattering of Multiple Laser Beams Sharing Acoustic Waves

C. Neuville,[1] V. Tassin,[1] D. Pesme,[2] M.-C. Monteil,[1] P.-E. Masson-Laborde,[1] C. Baccou,[3] P. Fremerye,[1] F. Philippe,[1] P. Seytor,[1] D. Teychenné,[1] W. Seka,[4] J. Katz,[4] R. Bahr,[4] and S. Depierreux[1]

[1]*CEA, DAM, DIF, F-91297 Arpajon, France*

[2]*Centre de Physique Théorique, UMR 7644, CNRS-Ecole Polytechnique, 91128 Palaiseau cedex, France*

[3]*LULI, UMR 7605 CNRS-Ecole Polytechnique-CEA-Université Paris VI, 91128 Palaiseau cedex, France*

[4]*Laboratory for Laser Energetics, University of Rochester, 250 East River Road, Rochester, New York 14623-1299, USA*

(Received 20 October 2015; revised manuscript received 10 April 2016; published 8 June 2016)

The indirect-drive scheme to inertial confinement fusion uses a large number of laser beams arranged in a symmetric angular distribution. Collective laser plasma instabilities can therefore develop that couple all the incident laser waves located in a cone to the daughter wave growing along the cone symmetry axis [D. F. DuBois *et al.*, Phys. Fluids B **4**, 241 (1992)]. With complementary diagnostics of Thomson scattering and of the scattered light, we demonstrate the occurrence of collective stimulated Brillouin sidescattering driving collective acoustic waves in indirect-drive experiments.

DOI: 10.1103/PhysRevLett.116.235002

The indirect-drive scheme to inertial confinement fusion relies on the conversion of the laser energy into x rays inside a high-Z cylindrical enclosure (or *Holhraum*) [1]. The resulting radiation drive then implodes the nuclear fuel capsule placed in the center of the *Holhraum*. In this irradiation scheme, the laser energy is delivered to the target through a large number of beams crossing each other in a small plasma volume $\sim(500\ \mu\mathrm{m})^3$ at the entrance of the *Holhraum*. The thorough control of the nonlinear behavior of these beams in the successive plasmas they traverse before being converted into x rays at the inside walls is crucial in order to optimize the coupling of the laser energy to the target. In the indirect-drive experiments, the individual beam intensity is typically above threshold for stimulating single-beam backscattering instabilities [2] whose regions of development may superimpose in the crossing-beam volume [3–8]. The multiple-plasma configuration may further modify the single-beam scattering instabilities [9–12]. In addition, the ponderomotive beating of each pair of crossing beams drives an enhanced ion acoustic wave (IAW). The subsequent induced stimulated Brillouin sidescattering (SBS) instability, in which the first laser wave couples with the driven IAW to scatter the light into the second laser wave, produces an exchange of energy between the two crossing beams [13–17] that leads to a redistribution of the forward going energy.

In the indirect-drive irradiation scheme, where the laser beams are angularly distributed in a highly symmetric configuration, a different type of multiple-beam instability may also develop in the crossing-beam region. This instability involves multiple laser beams located in a cone that collectively couple to a common daughter wave growing along the cone symmetry axis [18]. The collective nature of this coupling results in a reduction of the individual beam intensity threshold, and in an increase of the growth gain with the increase of the number of interacting laser beams. This collective instability also produces energy losses in new backward directions.

In this Letter, we demonstrate for the first time the occurrence of SBS corresponding to such collective IAW instabilities in indirect-drive experiments. This instability corresponds to the case where all laser beams incident in a cone amplify the same IAW, aligned along the cone symmetry axis, through stimulated Brillouin sidescattering. It was observed in indirect-drive experiments carried out with 15 crossing beams distributed in two incident laser beam cones with a geometry representative of the megajoule facilities. Enhanced level of IAWs have been measured along the symmetry axis of three cones made of four, six, and ten beams with complementary diagnostics of Thomson scattering (TS) and scattered light measurements. Similar physics of multibeam SBS had been previously investigated in experiments [19] in the context of direct drive in plasmas including a critical density surface. Collectively driven IAW may have developed in these previous experiments, but their effect was masked by the strong electromagnetic seeding of back- and sidescattering SBS by the light reflected at the critical surface [20]. In the *Hohlraum* geometry of the experiment reported in this Letter, the sidescattering of a first beam in the backward direction of a second crossing beam could be seeded by the backscattering of the second beam produced in the *Hohlraum* interior. Here, the plasma parameters in the region of crossing beams were measured with time-resolved Thomson scattering, allowing us to experimentally determine the geometry of sidescattering that drives the enhanced IAWs observed in the scattered-light measurements. This made possible the identification of the contribution of the collective Brillouin instability in this

diagnostic. This collective SBS instability is shown to produce significant scattered light losses in novel backward directions.

The experiments were carried out on the 351-nm Omega laser facility at the University of Rochester. The interaction was studied at the laser entrance hole (LEH) of rugby-ball-shaped *Holhraums* [21,22] filled with a 1-atm methane gas. A spherical capsule was mounted at the center of the *Hohlraum*. The revolution axis of the *Hohlraum* was aligned along the *P*5–*P*8 axis of the Omega target chamber. Twenty laser beams were incident on each side of the target distributed along three cones [see Fig. 1(a)]: five beams, at 21° from the axis, were pointed at 500 μm from the window outside the *Hohlraum*; similarly, five beams at 42° and ten beams at 59° were pointed at the LEH. The beams were focused by $f/6.7$ lenses through random-phase plates producing focal spots with a diameter of 300 μm full width at half maximum (FWHM). The laser pulse, with a total duration of 2.5 ns, was made of a prepulse of intensity $\sim 8 \times 10^{13}$ W cm^{-2} per beam followed by a main pulse for $t = 1.8$ to $t = 2.3$ ns at an intensity per beam of 5×10^{14} W cm^{-2}.

The crossed-beam interaction was studied with the 42° and 59° cones that superimposed in the region of LEH. The angular distribution of these 15 beams around the *Hohlraum* axis is schematically shown in Fig. 1(b), together with some of the collective IAWs that could grow in the volume of the crossing beams. A total of 17 cones, implying four to ten beams, are present in the crossing-beam volume [see Fig. 1(b)]. In particular, (*a*) two common IAW can be excited along the *Hohlraum* axis by the interaction of the five beams of the 42° cone and the interaction of the ten beams of the 59° cone (IAWa); (*b*) and (*c*) two distinct cones, with cone angles $\sim 50° - 40°$ are made of six and four beams having a symmetry axis at 10° (IAWb) and 35° (IAWc) from the *Hohlraum* axis, respectively; (*d*) a cone with the cone angle 20° is made of two beams of the 42° cone and two beams of the 59° cone (IAWd). The other cones are found by applying the $2\pi/5$ symmetry of the beams, so that they have an identical geometry. Three of these IAWs were observed in the experiment through TS and measurements of the scattered light in the Brillouin range.

The Thomson probe beam, converted to the fourth harmonics ($\lambda_{\text{probe}} = 263$ nm) and delivering 100 J in a pulse shape similar to the one used on the 351-nm beams, was incident in *P*9 and focused with an $f/6.7$ lens producing a 50-μm spot size. The Thomson scattered light was collected in an aperture angle of 5.7° in the direction of *P*7 by a telescope [23]. The scattering angle measured between the directions of the probe and scattered light is $\theta_{\text{TS}} = 60°$, so that the probed IAWs have wave vectors $k_{\text{IAW,TS}} = 2\ k_p\ \sin(\theta_{\text{TS}}/2)$ with $k_p = 2\pi/\lambda_{\text{probe}}$. Time-resolved spectra with resolutions of 80 ps and 0.4 Å were then obtained with the combination of a spectrometer and a streak camera. This diagnostic was first used to experimentally measure the plasma expansion velocity and the acoustic velocity [24] at two locations along the *Hohlraum* axis: (i) in the region of the crossing beams and (ii) at a distance of 300 μm outside the *Hohlraum*. These results are shown as a function of time in Fig. 2.

The IAWs probed by the TS diagnostic are at 35° from *P*8 and along the axis of the cone formed by beams 12, 23, 57, and 62 [see Fig. 1(c)]. The IAW (IAWc) driven by SBS of the 351-nm beams along the axis of this cone has a wave vector $k_{\text{IAW,SBS}} = 2\ k_0\ \cos(42°)$ with $k_0 = 2\pi/351$ nm, so that $k_{\text{IAW,SBS}} \approx k_{\text{IAW,TS}}$. As a result, for the *Hohlraum* aligned along the *P*5–*P*8 axis, the IAW probed by TS that propagates towards the *Hohlraum* matches in direction and wave vector [see Figs. 1(d) and 1(c)] to IAWc. A typical time-resolved TS spectrum measured in the beam-crossing region is displayed in Fig. 3(a). The power scattered off the IAW [defined as IAW1 in Fig. 1(d)] propagating towards the *Hohlraum* is

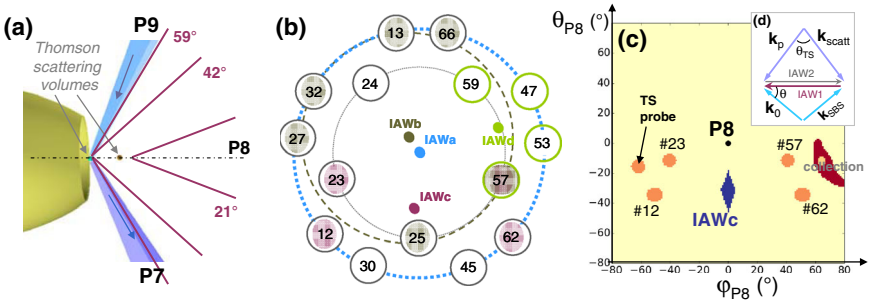

FIG. 1. (a) Representation of the LEH showing the three cones of heater beams and the geometry of the TS diagnostic. (b) Schematic view of the 15 interaction beams around the *Hohlraum* axis. The directions of the IAWs driven by the laser beams of four representative cones are drawn. IAWa is the IAW excited along the *Hohlraum* axis by the ten beams of the 59° cone, IAWb is excited by beams 13, 66, 27, 32, 25, and 57, IAWc is excited by beams 12, 23, 57, and 62, and IAWd is along the axis of the cone formed by beams 47, 53, 57, and 59. (c) Directions of IAWc (in blue) such that it is amplified by the same SBS geometry for the four surrounding beams and angular distribution (in red) of the Thomson scattered light calculated for an electronic density of $0.1 n_c$ (n_c is the critical density for the 351-nm beams). (d) Thomson scattering geometry for probing the common ion acoustic wave (IAW1) driven along the axis of a 42° cone of 351-nm interaction beams with a 263-nm probe.

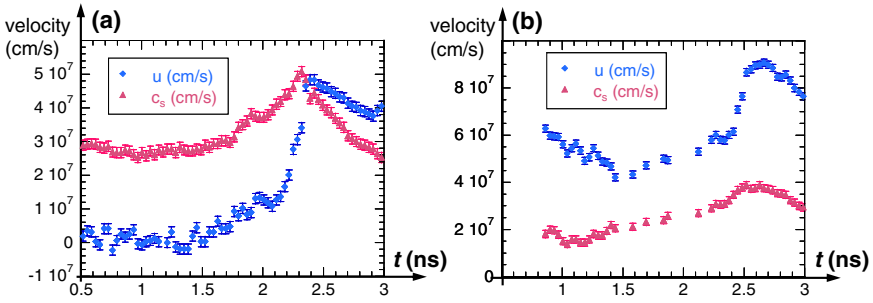

FIG. 2. Expansion velocity (u) and acoustic velocity (c_s) measured (a) in the spatial domain of beam crossing and (b) at 300 μm outside the *Hohlraum*.

higher than the power scattered off the opposite IAW during the time period [1.7 ns, 2.3 ns], corresponding to the time interval during which the heater beams were close to their maximum intensity [see Fig. 3(b)]. No increased signal was observed when the TS volume was located outside the crossing-beam region. This shows that the crossing-beam interaction of the heaters enhances the level of an IAW having the direction and wave number of IAWc.

The scattered light was collected in the backward direction of one beam of the 59° cone (beam 30) and of one beam of the 42° cone (beam 25). It was then analyzed in time and wavelength with resolutions of 80 ps and 0.4 Å by the full-aperture backscattering stations (FABSs). These measurements allowed the diagnostic of the IAWs driven along the cone symmetry axis for a six-beam cone (IAWb) and a ten-beam cone (IAWa). For instance, the stimulated Brillouin sidescattered light of beam 13 off IAWb, which is the IAW driven along the axis of the cone formed by beams 13, 66, 25, 57, 27, and 32, was collected in the backward direction of beam 25. Time-resolved signals measured on the FABS diagnostics are shown in Figs. 4(a) and 4(b). For the time interval [1.8 ns, 2.3 ns], when the laser intensity was close to its maximum, two contributions were detected in each FABS. The first signal, starting at $t = 1.9$ ns in FABS25 and at $t = 1.8$ ns in FABS30, is due to Brillouin backscattering of the beam itself developing in the plasmas, made of the filling gas or gold wall, located inside the *Hohlraum*. In the two FABSs, this first component simply depended on the energy of the beam itself.

The origin of the second component, observed after $t = 2.2$ ns, is different as we observed that the variations, in time and amplitude, of this second signal were dependent on the energy fired on the other cone of crossing beams. As an example, the amplitude of this second signal measured in FABS30 was increased when the energy on the two cones was reduced below the threshold for the appearance of the second signal in FABS25. This competition between the second contribution measured in the two FABS indicates that this second signal grows in the region of the crossing beams. In this volume, whose plasma parameters were experimentally measured, the geometry of the scattering then uniquely determines the wavelength shift of the scattered light ($\Delta\lambda_{\mathrm{SBS}}$) that scales as $\Delta\lambda_{\mathrm{SBS}} \propto k_{\mathrm{IAW}} \propto \cos(\theta)$. The corresponding wavelength, calculated with the experimentally characterized plasma parameters in the case of the previously described scattering off IAWb by beam 13, is shown by the solid line as a function of time in Fig. 4(a) together with the time-resolved spectrum measured in the backward direction of beam 25. The second signal, observed after $t = 2.2$ ns, extends over a very narrow spectral range, corresponding exactly to the wavelength expected for the light scattered by beam 13 off IAWb. This second signal can thus be attributed to a SBS sidescattering instability having the geometry of the collective IAW instability that drives IAWb. The scattering losses in this second signal maximize at ~1%.

A similar analysis was made for the light collected in the backward direction of beam 30. In this diagnostic, we could

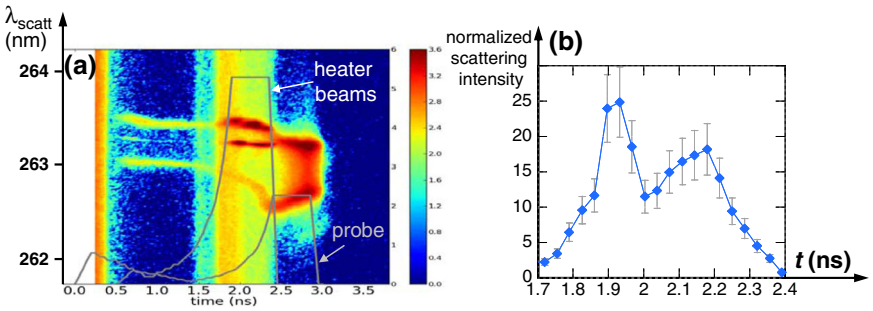

FIG. 3. (a) Time-resolved spectrum of the Thomson scattered light collected in the region of beam crossing. The pulse shapes of the probe beam and of the heater beams are shown in grey. (b) Time-resolved intensity of the light scattered off the IAW1, normalized to the intensity of the light scattered off the counterpropagating ion wave IAW2.

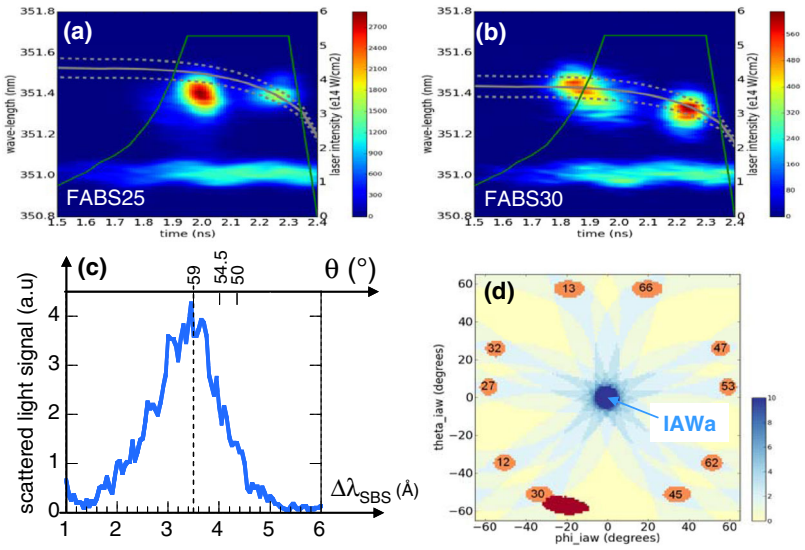

FIG. 4. (a) Time-resolved spectrum of the scattered light collected in the backward direction of beam 25. The solid grey line shows the wavelength calculated for the SBS of beam 13 in the collective instability that drives IAWb that is collected in the direction of FABS25. The two dashed lines represent the expected wavelength range for this scattered light, taking into account the aperture of the diagnostic and laser beams and the size of the crossing-beam volume. (b) Time-resolved spectrum of the scattered light collected in the backward direction of beam 30. As in (a), the grey lines represent the wavelength range calculated for the light scattered by beam 66 in the FABS30 direction off the collective IAWs driven along the *Hohlraum* axis by the ten-beam instability. (c) Scattered light wavelength for the signal measured in FABS30 at $t = 2.25 \pm 0.05$ ns. (d) The directions of the IAWs having equal wave vectors are shown with respect to the ten laser beams of the 59° cone that stimulate IAWa. A collective ion acoustic wave is driven in each of the directions where multiple beams contribute. In the direction indicated as IAWa, the ten beams amplify the corresponding IAW. The regions shown in red represent the directions of scattering of beam 66 off IAWa.

collect the SBS of beam 66 off IAWa, the IAW driven along the axis of the 59° cone. The calculated SBS wavelength shift is plotted on the corresponding spectrum in Fig. 4(b). The late-time contribution measured in FABS30 has its spectral features (narrow spectral range and wavelength value) corresponding to what is expected for the scattering off IAWa.

The observation of a sidescattering signal peaked in wavelength is a strong indication of multiple-beam effects, as any of the beams could contribute in the FABS to produce single-beam sidescattered SBS with a large variety of angles and scattered light wavelengths. Rather, in the experiment, only sidescattering with the largest angle was observed. This demonstrates that the sidescattering of individual beams is negligible. In contrast, the single-beam SBS scattering off the IAW driven along the cone axis yields a significant signal. In the geometry of the experiment, the level of this IAW located along the symmetry axis can be enhanced by the beating of an incoming laser beam with the Brillouin light backscattered by the symmetric beam in the *Hohlraum* interior. This could happen because the cones of beams around the three diagnosed IAWs include pairs of beams symmetric with respect to the cone axis. However, in our experiment, such a two-beam electromagnetic seeding could develop not only for opposed beams but also between any pair of crossing beams providing the beating of incoming and backscattered lights matches for the resonance of the IAW driven in the specific geometry. Consequently, it could hardly explain the sharp signal measured in the FABS. This situation strongly differs from the electromagnetic seeding encountered in the experiment by Seka *et al.* [19], in which the seeding occurred through reflection at the critical surface and could thus develop only for beams symmetric with respect to the target normal.

The collective amplification of SBS in the crossing-beam region, possibly seeded by the previously described beating, accounts for the measured SBS spectrum at late time. The wavelength of the scattered light measured in FABS30 for $t = 2.25 \pm 0.05$ ns is shown in Fig. 4(c). Its FWHM of 1.4 Å is consistent with the amplification of SBS with $\theta = 59°$ over a length of 75 μm along the *Hohlraum* axis combined with the spectral resolution of the diagnostic (0.4 Å). This 75-μm length corresponds to the region of maximum overlap intensity for the ten beams. At $\theta = 59°$, the full aperture of the ten beams contributes to the amplification of IAWs with the same wave vector. The ten beams can also amplify the same IAWs for $\theta = (59 \pm 4)°$, but less amplification is possible because only part of the rays contributes for each beam. It produces an additional broadening of ± 0.4 Å in the spectrum. For the scattering of beating IAWs, two beams (beams 13 and 47) are found with slightly different angles than for beam 66 and could contribute at $\theta = 54.5°$. However, the

measured spectrum is rather symmetric with respect to $\Delta\lambda_{SBS} = 3.5$ Å, showing that the scattering with angles θ smaller than 59° do not contribute significantly to the measured signal. Only sidescattering that implies the IAW to which multiple beams are contributing can be observed. A similar analysis gives the same conclusion for the measurements in FABS25. This demonstrates that the collective amplification or reamplification of SBS light in the crossing-beam region largely dominates over the electromagnetic seeding, possibly followed by a single-beam reamplification.

The absolute energy measurements performed in the FABS made possible the evaluation of the energy losses due to the collective SBS instability of the 59° cone. To do so, we first consider the geometry of the scattering, taking into account the aperture of the beams and of the diagnostic. The geometry of the SBS of beam 66 in the collective instability that drives the IAW along the *Hohlraum* axis (IAWa) is shown in Fig. 4(d) assuming straight-line propagation of the light in front of the crossing-beam region at LEH. Its analysis shows that only a small fraction ($<1/10$) of this scattered light falls in the aperture of beam 30 and is collected in its backscattering station. In FABS30, the signal associated with the collective instability peaks at ~3% of the laser power per beam. From Fig. 4(d), an additional significant fraction of the light is expected to be scattered with larger angles. This was confirmed in complementary experiments where light with the same spectral feature at late time was detected at ~20° of a beam of the 59° cone. So, for the ten-beam instability, we estimate that the scattering losses may be ten times higher than those measured in FABS30.

The physics of multiple crossing beams has been studied at the laser entrance hole of indirect-drive targets with Thomson scattering and scattered light measurements. The experiments have been performed with 15 crossing beams arranged in two cones in a geometry representative of the megajoule facilities. Levels of fluctuations increased above thermal noise have been observed for the ion acoustic waves aligned along the axis of the cones made of four, six, and ten beams. A total of 17 such cones were identified for the angular distribution of the beams used in the experiment. All the resultant IAWs excited in the volume of the crossing beams may impact the crossed-beam energy transfer that takes place in the same spatial region [25,26]. The collective Brillouin sidescattering of multiple beams was clearly identified as being responsible for the enhancement of the IAWs driven along the axis of the six- and ten-beam cones. This collective Brillouin instability was amplified in a well-defined geometry of sidescattering in a small region defined by the maximum intensity of the crossing beams, resulting in a scattered light signal strongly peaked in wavelength. This scattered light was associated with significant energy losses in novel backward directions. These collective Brillouin scattering instabilities could significantly impair the laser-target coupling in indirect-drive experiments.

This work was partly performed in the framework of the ANR project ILPHYGERIE (Project No. ANR-12-BS04-0006-01). We gratefully acknowledge fruitful discussions with C. Labaune, M. Casanova, S. Hüller, P. Loiseau, D. Benisti, A. Heron, C. Riconda, V. Tikhonchuk, and A. Debayle.

[1] J. D. Lindl, Phys. Plasmas **2**, 3933 (1995).
[2] W. L. Kruer, *The Physics of Laser Plasma Interactions* (Addison-Wesley, Redwood City, CA, 1988).
[3] H. A. Baldis, C. Labaune, E. Schifano, N. Renard, and A. Michard, Phys. Rev. Lett. **77**, 2957 (1996).
[4] C. Labaune, H. A. Baldis, B. Cohen, W. Rozmus, S. Depierreux, E. Schifano, B. S. Bauer, and A. Michard, Phys. Plasmas **6**, 2048 (1999).
[5] R. K. Kirkwood *et al.*, Phys. Plasmas **18**, 056311 (2011).
[6] D. E. Hinkel *et al.*, Phys. Plasmas **18**, 056312 (2011).
[7] R. K. Kirkwood *et al.*, Plasma Phys. Controlled Fusion **55**, 103001 (2013).
[8] J. F. Myatt *et al.*, Phys. Plasmas **21**, 055501 (2014).
[9] J. C. Fernández *et al.*, Phys. Rev. Lett. **81**, 2252 (1998).
[10] S. Depierreux *et al.*, Nat. Commun. **5**, 4158 (2014).
[11] V. Yahia *et al.*, Phys. Plasmas **22**, 042707 (2015).
[12] D. Turnbull, P. Michel, J. E. Ralph, L. Divol, J. S. Ross, L. F. B. Hopkins, A. L. Kritcher, D. E. Hinkel, and J. D. Moody, Phys. Rev. Lett. **114**, 125001 (2015).
[13] W. L. Kruer, S. C. Wilks, B. B. Afeyan, and R. K. Kirkwood, Phys. Plasmas **3**, 382 (1996).
[14] V. V. Eliseev, W. Rozmus, V. T. Tikhonchuk, and C. E. Capjack, Phys. Plasmas **3**, 2215 (1996).
[15] C. J. McKinstrie, J. S. Li, R. E. Giacone, and H. X. Vu, Phys. Plasmas **3**, 2686 (1996).
[16] P. Michel *et al.*, Phys. Plasmas **17**, 056305 (2010).
[17] J. D. Moody *et al.*, Nat. Phys. **8**, 344 (2012).
[18] D. F. DuBois, B. Bezzerides, and H. A. Rose, Phys. Fluids B **4**, 241 (1992).
[19] W. Seka, H. A. Baldis, J. Fuchs, S. P. Regan, D. D. Meyerhofer, C. Stoeckl, B. Yaakobi, R. S. Craxton, and R. W. Short, Phys. Rev. Lett. **89**, 175002 (2002).
[20] C. J. Randall, J. R. Albritton, and J. J. Thomson, Phys. Fluids **24**, 1474 (1981).
[21] M. Vandenboomgaerde, J. Bastian, A. Casner, D. Galmiche, J.-P. Jadaud, S. Laffite, S. Liberatore, G. Malinie, and F. Philippe, Phys. Rev. Lett. **99**, 065004 (2007).
[22] F. Philippe *et al.*, Phys. Plasmas **21**, 074504 (2014).
[23] J. Katz *et al.*, Rev. Sci. Instrum. **83**, 10E349 (2012).
[24] J. Sheffield, *Plasma Scattering of Electromagnetic Radiation* (Academic Press New York 1975).
[25] B. I. Cohen, B. F. Lasinski, A. B. Langdon, E. A. Williams, H. A. Baldis, and C. Labaune, Phys. Plasmas **5**, 3402 (1998).
[26] P. Michel, W. Rozmus, E. A. Williams, L. Divol, R. L. Berger, R. P. J. Town, S. H. Glenzer, and D. A. Callahan, Phys. Rev. Lett. **109**, 195004 (2012).